European Heart Journal – Cardiovascular Imaging (2016) **17**, 596–603
doi:10.1093/ehjci/jew079

REVIEW

EuroEcho-Imaging 2015: highlights

Julien Magne[1,2]*, Bogdan A. Popescu[3], Bernard Cosyns[4], Erwan Donal[5], Owen Miller[6], Danilo Neglia[7], Sven Plein[8], Patrizio Lancellotti[9,10], and Gilbert Habib[11,12]

[1]CHU Limoges, Hôpital Dupuytren, Service Cardiologie, F-87042 Limoges, France; [2]INSERM 1094, Faculté de médecine de Limoges, 2, rue Marcland, 87000 Limoges, France; [3]University of Medicine and Pharmacy 'Carol Davila'—Euroecolab, Institute of Cardiovascular Diseases 'Prof. Dr. C. C. Iliescu', Bucharest, Romania; [4]UZ Brussel-CVHZ, 1090 Brussels, Belgium; [5]CIC-IT 1414, CHU Rennes, Université Rennes 1, Service de Cardiologie, CHU RENNES, Rennes, France; [6]Department of Congenital Heart Disease, Evelina London Children's Hospital, London, UK; [7]Fondazione CNR/Regione Toscana G. Monasterio, Pisa, Italy; [8]Multidisciplinary Cardiovascular Research Centre and Leeds Institute of Cardiovascular and Metabolic Medicine, University of Leeds, Leeds, UK; [9]Departments of Cardiology, University of Liège Hospital, GIGA Cardiovascular Sciences, Heart Valve Clinic, CHU Sart Tilman, Liège, Belgium; [10]Gruppo Villa Maria Care and Research, Anthea Hospital, Bari, Italy; [11]Department of Cardiology, Aix-Marseille Université, Marseille 13284, France; and [12]La Timone Hospital, 13005 Marseille, France

Received 21 March 2016; accepted after revision 22 March 2016; online publish-ahead-of-print 20 April 2016

The annual meeting of the European Association of Cardiovascular Imaging, EuroEcho-Imaging, was held in Seville, Spain, in December 2015. In the present paper, we present a summary of the 'Highlights' session.

Keywords heart failure • heart valve disease • 3D echocardiography • cardiac magnetic resonance • congenital heart disease • nuclear cardiology • cardiac computed tomography

Introduction

The nineteenth annual scientific meeting of the European Association of Cardiovascular Imaging (EACVI), EuroEcho-Imaging 2015, was held in Seville, Spain. The main themes were 'cardiomyopathies' and 'early diagnosis of cardiovascular disease'. The meeting was a great success with a high number of participants (>3100 delegates) and over 1100 abstracts and 150 clinical cases submitted. Overall, 126 abstracts or clinical cases were accepted as oral presentation, and 54 moderated posters were presented. Of note, the preferred topics regarding abstracts submission were 'valvular heart diseases', 'cardiomyopathies', 'tissue Doppler and speckle tracking', 'systemic disease', and 'assessment of systolic function'.

On the last day of the meeting, the 'Highlights' session wrapped up the event with a summary of the most relevant abstracts presented throughout the congress. A short report of this session is presented below.

Heart failure

B-lines evaluated by lung ultrasound are a sonographic sign of pulmonary interstitial oedema, which can be detected in patients with increased extravascular lung water, a well-known determinant of prognosis in heart failure (HF).[1] A prospective cohort of 89 patients admitted to a cardiology department for dyspnoea and/or clinical suspicion of HF was enrolled and followed up for 6 months. B-lines were evaluated with a cardiac probe on the anterolateral chest, at admission (T0) and at discharge. Feasibility of B-lines assessment was excellent (100%), and the time required was <5 min in all cases. Average B-lines significantly decreased from T0 to discharge (from 53 ± 48 to 23 ± 23, $P < 0.0001$). The 6-month event-free survival was significantly better in patients with lower number of B-lines ($P < 0.0001$) and on multivariate analysis. A high number of B-lines (i.e. >15) (hazard ratio = 10.3, 95% confidence interval: 2.3–45.6) was a powerful independent predictor of impaired outcome, stronger than any other echocardiographic or clinical parameters.

In regard to RV function assessment using echocardiography, there is no consensus on the most appropriate strain parameter. In 103 patients, global longitudinal strain (RV-GLS) and free wall longitudinal strain (FWLS)[2] were compared regarding event-free survival using Kaplan–Meier analysis. Patients with RV-GLS > −17.3% showed lower event-free survival rate ($P < 0.001$), and this seems to depict better prognostic value than FWLS. In multivariate analysis including both strain parameters, only RV-GLS > −17.3% was associated with outcome.

Left ventricular (LV) pressure–strain loops (PSLs) have been validated as a non-invasive index of myocardial performance and compared with FDG-PET.[3] Regional LV pressure longitudinal strain loops allow the assessment of global and regional myocardial performance. Their relationship with LV dyssynchrony provides a window for a better understanding of LV mechanics. Also, 3-dimensional (3D)

* Corresponding author. Tel: +33 62 40 42 361; Fax: +33 55 50 56 334. E-mail: jul.magne@yahoo.fr

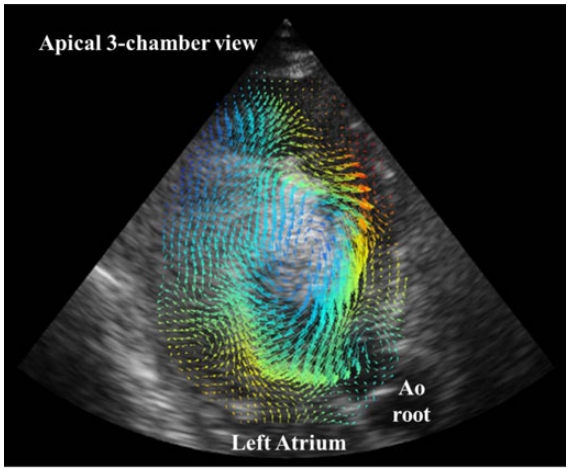

Figure 1 Example of the left ventricular fluid dynamics assessed by Echocardiographic Particle Image Velocimetry (Echo-PIV). This approach looks very promising to optimize the mode of pacing in patients implanted with a bi-ventricular pace maker and with a left ventricular multi-pole lead.

echocardiography and particle image velocimetry (Echo-PIV) were performed for different biventricular pacing settings (*Figure 1*).[4] Flow force angle (FFA) by Echo-PIV reflected the dominant direction of blood flow momentum (0° when flow forces are parallel with LV long axis, and 90° when flow forces are transversal). Accordingly, a lower FFA would reflect more efficient blood flow dynamics within the LV. FFA by Echo-PIV was significantly lower for BIV vs. CRT-OFF, and also for MPP vs. BIV. 3DE and Echo-PIV enabled to identify an acute improvement in LV systolic function and blood flow dynamics during MPP.[5]

Patients with severe HF and ejection fraction ≤35% represent a heterogeneous group. Strain parameters derived from LV speckle tracking echocardiography (STE) could reflect residual functional capacity and haemodynamic compromise better than ejection fraction (EF). LV GLS was better correlated with 6-min walking test (MWT) distance and brain natriuretic peptide (BNP) levels than LV ejection fraction. In multiple linear regression analysis, GLS emerged as a determinant of 6-MWT distance and BNP level.[6]

In HF with preserved ejection fraction (HFpEF), the exercise intolerance is determined by multiple mechanisms. In a study from Poland, peak VO_2 and exertional reserve were less impaired in patients with normal vs. patients with abnormal *E*/*e*′ ratio.[7] Independent correlates of peak VO_2 were exertional *E*/*e*′ ratio and LV GLS. Nevertheless, there is still no consensus for the diagnosis of HFpEF.[8] Current studies recommend stress echocardiography protocols, but single standard peak or timing measurements are limited due to the complexity of this disease. The contribution of a combined analysis of multiple myocardial velocity patterns and their relative relevance for the characterization of HFpEF were investigated. The characterization of HFpEF is improved by a combined analysis of multiple velocity traces from stress echo studies using machine learning. The method suggests additional features of interest to be used in clinical diagnosis.

Valvular heart disease

The majority of abstracts selected this year in the valvular heart disease section of the highlights session investigated the impact and relationship between concomitant valve regurgitation (i.e. MR or TR) and transcatheter aortic valve intervention (TAVI). Indeed, the presence and severity of TR, as well as RV function, were retrospectively assessed in 519 patients with TAVI.[9] Only 11% of patients were found with ≥moderate TR at the time of TAVI and TAPSE, and not TR severity was an independent predictor of mortality following TAVI. However, in around 50% of patients, TR did not improve after TAVI, and persistent TR at 6 months was independently associated with reduced survival. Furthermore, the lack of improvement of TR following TAVI was mainly determined by older age, female gender, history of atrial fibrillation, and pulmonary hypertension.

Discrepant results were reported regarding the impact of MR on outcome following TAVI. A study by Del Val Martin *et al.*[10] reported the prospective analysis of 90 patients with TAVI. More than moderate MR was found in 24% of patients before TAVI and decreased after TAVI (8%), without statistically significant difference between patients with significant vs. non-significant MR improvement in terms of 2-year clinical event (26.8 vs. 24.3%). Conversely, Szymanski *et al.*[11] have reported a larger population of 381 patients with TAVI in whom both significant pre-TAVI and post-TAVI MR were associated with significantly reduced 1-year survival.

The role of LV GLS in patients with severe aortic stenosis (AS) and preserved LV ejection fraction is growing. In 582 patients included in a multicentre study,[12] GLS > −13.75%, assessed using 2D STE, was a significant determinant of reduced 2-year survival (93 vs. 84%, $P = 0.001$). In addition, after adjustment of confounders, impaired LV GLS was associated with around 2.5-fold increase in risk of death (hazard ratio = 2.47, 95% confidence interval: 1.04–5.90, $P = 0.041$). Patients with atrial fibrillation (AF) may develop atrial functional mitral regurgitation (AFMR) despite normal ventricular function. Tang *et al.*[13] performed a real-time 3D echocardiographic study evaluating 3D mitral annular geometry and dynamics in AF patients. They aimed to identify factors, including LA and LV function parameters, associated with abnormalities of mitral annular dynamics in AFMR. They found that impaired pre-systolic contraction and saddle shape deepening of mitral annulus may contribute to AFMR. Furthermore, compared with patients without AFMR, those with AFMR depicted significantly lower left atrial peak strain (20 ± 8 vs. 12 ± 6%, $P < 0.0001$) and LV basal circumferential strain (−19 ± 5 vs. −16 ± 3%, $P = 0.002$). Consequently, their data suggest that the loss of pre-systolic annular deformation is associated with impaired contractile function of the left atrium and basal LV myocardium.

Histotripsy is a cavitation-based therapy (i.e. using mechanical effect) that uses very short, high-pressure ultrasound pulses to generate a dense, energetic, lesion-producing bubble cloud (*Figure 2*). A pilot, proof-of-concept study was conducted by Villemain *et al.*[14] in which they applied histotripsy for non-invasive mitral valve chordal cutting both in vitro using explanted sheep heart ($n = 10$) and in vivo on sheep beating heart after sternotomy ($n = 7$). The in vitro study showed excellent feasibility with 100% of chordal cut in an average time to complete section of 5.5 min (range: 3–9 min). Similar results were reported in the in vivo study in terms of feasibility but with longer average procedure time (21 min). Of interest, the

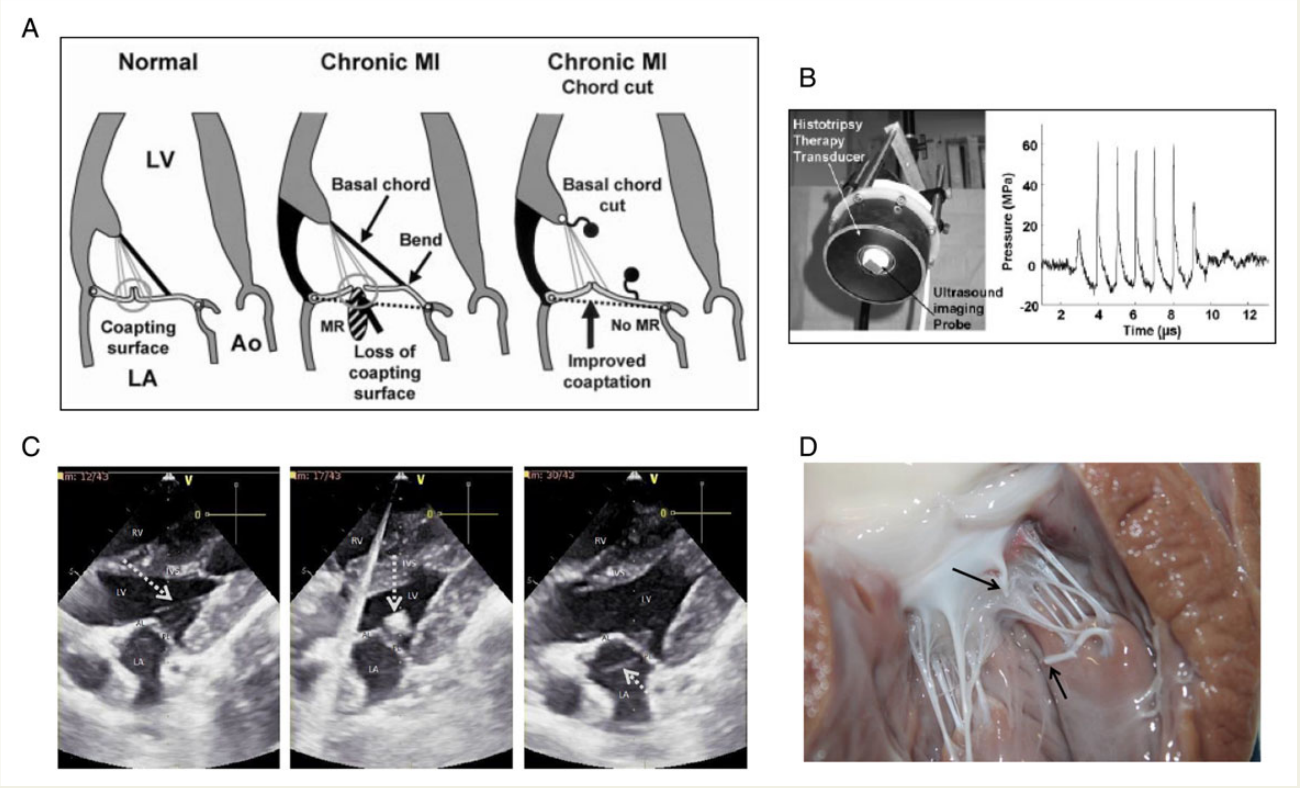

Figure 2 Histotripsy application for mitral chordal cutting. (*A*) Description of chordal cutting mechanism. (*B*) Histotripsy device. (*C*) Two-chamber epicardial echocardiography imaging. Left, before chordal cutting. Centre, during the therapy with cavitation bubbles observed on the basal chordae of the anterior leaflet (white arrow). Right, after therapy with basal chordae prolapsing into the left atrium (with arrow). (*D*) En-face view of the explanted mitral valve apparatus. We observed the section of the basal chordae arising from the anterior leaflet and inserting on the posterior papillary muscle (black arrow).

sectioned chordae were visible on echocardiography, and mitral valve coaptation remained normal with no significant MR. Anatomical and histological post-mortem explorations of hearts confirmed the section of the chordae and only one additional anatomic lesion on LV lateral wall. The authors concluded that histotripsy may achieve successful mitral valve chordal cutting and that this technique may open the door to the non-invasive treatment of functional MR.

3-Dimensionnal echocardiography

A patient-specific, quantitative model of the complex 3D mitral valve (MV) geometry and dynamics might improve pathophysiologic insight and enhance therapeutic efficacy by predicting the effect of interventions. A patient-specific numerical model of the MV apparatus based on 3D transoesophageal echocardiography (3D-TEE) was developed and validated in predicting MV dynamics in different haemodynamic loading conditions (*Figure 3*).[15] The model realistically predicted opening and closure of the MV leaflets in all datasets. Comparison of the predicted mid-systolic closure vs. real-time 3D-TEE imaging showed good accuracy with an average prediction error (root mean square) ranging from 1.4 to 2.9 mm. Furthermore, the position of the coaptation line was predicted with an average error ranging from 0.6 to 2.0 mm. Point-to-point error between predicted and real-time leaflet position was the highest in the intertrigonal area due to bulging in the simulated leaflets. 3D-TEE-based patient-specific numerical MV modelling allows a realistic prediction of valvular dynamics in physiological loading conditions.

The analysis of the mitral annulus (MA) 3D geometry was performed and compared between 71 patients with primary mitral regurgitation (MR) due to fibroelastic deficiency and controls. Patients were classified according to the extent of MV disease, i.e. limited MV disease $\leq$3 scallops affected vs. extensive MV disease, i.e. $\geq$4 scallops involved (Barlow-like).[16] The MA diameters and the non-planar angles (NPA) were measured in five systolic moments throughout systole. The parameters describing MA non-planarity were significantly different between patients with fibroelastic deficiency, Barlow-like disease and normal subjects mostly in the late part of systole suggesting the importance of non-planar angle changes in the pathophysiology of different types of MV prolapse.

The study of Aquila *et al.*[17] aimed to evaluate the feasibility and accuracy of a full-automated software for 3D TEE assessment of MV in 45 patients with severe primary and secondary MR. The software correctly identified anatomic differences in primary vs. secondary MR. Furthermore, the diameter enlargement in diastole suggested that in the primary MR, the annulus has a dynamic behaviour that is profoundly different from the non-dynamic annulus observed in secondary MR.

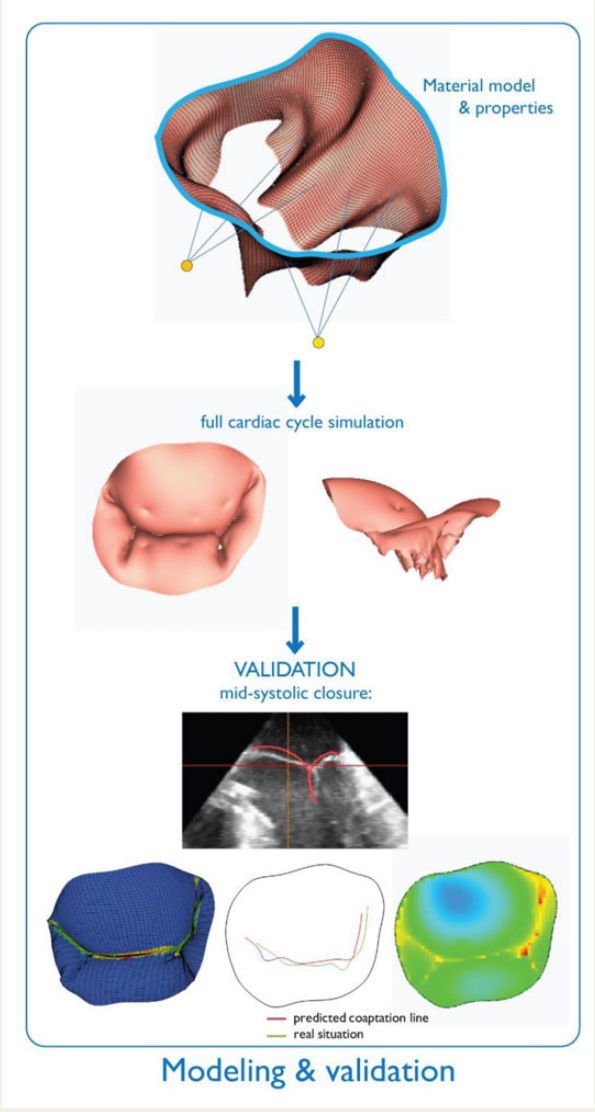

Figures 3 Geometry of the mitral valve (MV) apparatus extraction from full volume 3D-TEE by manual segmentation of one end-diastolic frame and transferred into a finite element mesh. Patient-specific boundary conditions (annular and papillary muscle position and dynamics) were manually extracted from the 3D-TEE images for the entire cardiac cycle. Leaflets were modelled as transversely isotropic hyperelastic material based on prior *in vitro* mechanical testing; chordae were modelled as hyper elastic connections between papillary muscles and leaflets. The end-diastolic finite element mesh, material properties, and boundary conditions were combined to numerically calculate MV dynamics when applying a certain haemodynamic load. For validation, datasets from five normal MVs were prospectively collected during elective percutaneous closure procedures of a patent foramen ovale during which left atrial and ventricular pressures were invasively measured, and 3D TEE was simultaneously acquired.

Estimation of mitral valve area (MVA) by using the PISA method with real-time 3D color Doppler echocardiography might circumvent the technical limitations of 2D echocardiography planimetry. In patients with mitral stenosis, the calculation of the flow convergence volume by 3D and the PISA-derived estimate of MVA was performed using a semi-automatic dedicated software. The use of 3D PISA showed the best correlation, followed by pressure half-time, continuity equation, and 2D PISA. Therefore, it was suggested that MVA estimation using 3D PISA method was feasible and more accurate than 2D methods.[18]

Unfortunately, limited data are available regarding 3D STE to evaluate LV mechanics in neonates. The aims of this study were to evaluate the feasibility and establish normal values of 3D LV volumes, ejection fraction, and the four normal strains in 50 healthy neonates.[19] While naturally sleeping, full volume data sets from the apical window were acquired. Mean indexed LV diastolic, systolic volumes, and ejection fraction were 24.7 $\pm$ 3.6 mL/m^2, 9.2 $\pm$ 1.3 mL/m^2, and 63 $\pm$ 3.7%, respectively. Normal global longitudinal, circumferential, radial, and tangential 4D strain were -20.9 ± 2.8, -32.4 ± 3.1, 44.3 $\pm$ 3.4, and -39.7 ± 3.4%, respectively. The 3D-STE is feasible in newborns without the need for sedation and allows establishing normal reference values of regional and global LV 4D strain and volumes.

Cardiovascular magnetic resonance

Abstracts on cardiovascular magnetic resonance (CMR) imaging focused mostly on emerging CMR methodology and prognostic value of established methods.

Native T_1 mapping has been used to detect diffuse myocardial pathologies including oedema and fibrosis. Vieira *et al.* demonstrated in 20 adolescents and young adult cancer survivors that non-contrast CMR T_1 mapping can identify subclinical cardiac injury following anthracycline therapy, which was not detected by standard LV function assessment.[20] They also found changes in pulse wave velocity (PWV), suggesting that emerging CMR methods are candidates for future screening of cancer patients.

T_1 mapping before and after contrast administration can be used to quantify the myocardial extracellular volume (ECV), and several recent studies have indicated that ECV is a marker of interstitial fibrosis and infiltration in a wide range of conditions. Although normal values vary to some extent between previous reports, an ECV of 23–26% is generally considered as normal. Nastase *et al.* studied 27 consecutive patients with severe AS and 21 patients with severe aortic regurgitation (AR).[21] While native T_1 was similar between the two groups, ECV was elevated in both groups and was higher in patients with AR (31 $\pm$ 3%) than in patients with AS (29 $\pm$ 4%). These preliminary results clearly require confirmation in larger studies but point to the potential of parametric CMR mapping to identify LV remodelling in valve disease with the potential to contribute to decisions about the timing of surgery.

Another abstract in aortic valve disease by von Knobelsdorff *et al.*[22] examined the value of CMR tissue phase mapping in patients with LV pressure overload at rest and during stress. In this study, 9 patients with hypertensive heart disease, 24 patients with AS, and 41 healthy controls were studied. Hypertensive patients showed lower peak myocardial velocities in diastole, while those with AS had reduced velocities both in diastole and in systole compared with healthy controls. Furthermore, there was no adaption to isometric

exercise in either of the patient groups, unlike in controls, as an indicator for early functional impairment.

Castillo *et al.*[23] investigated the recently reported 'splenic switch-off' seen during vasodilators stress CMR studies. They showed in a small study that splenic perfusion was reduced with both adenosine and dipyridamole but not with dobutamine stress. The authors concluded that splenic perfusion assessment may be used to reduce false-negative stress CMR studies.

Several abstracts dealt with prognostic CMR markers. Park and co-workers assessed the use of CMR in the assessment of patients with TR, making use of the ability of CMR to accurately assess right ventricular size and function.[24] They studied 75 patients in whom severe functional tricuspid regurgitation was the only haemodynamically significant lesion and who underwent isolated tricuspid valve surgery. They report that right ventricular ejection fraction, derived from CMR, was an independent predictor of mortality.

Ramos *et al.*[25] studied 394 patients referred for adenosine perfusion CMR and investigated whether a blunted heart rate response to adenosine had prognostic implications. Although there were significant differences in death on follow-up depending on the heart rate response in groups divided into tertiles, there was no statistically significant difference on multivariate analysis. However, this work suggests that larger studies should be considered to further explore these relationships.

Congenital heart disease

The congenital heart disease (CHD) programme in 2015 featured many strong scientific sessions and a variety of abstracts spanning the whole life cycle from fetal cardiology to longer term outcomes in adults with single ventricle palliation for complex CHD.

The predominant themes that emerged among the accepted abstracts were aortic dilatation either in patients born with congenital bicuspid aortic valve (BAV) or with other forms of CHD, most notably Tetralogy of Fallot; multimodality and integrated assessment for patients with repaired CHD; and assessment and surgical planning for newborns, children and adults with complex single ventricle CHD.

In a retrospective study of 81 adults with BAV, Aguiar Rosa *et al.*[26] aimed to identify predictors of aortic dilatation by exploring any relationship between aortic dilation and BAV subtype, transaortic valve gradient, AR, and/or global circumferential strain (GCS) at the level of the valve annulus. The commonest BAV pattern seen was fusion of the right and left coronary cusps in 53% of cases. This is in general agreement with other abstracts presented at the meeting.[27,28] Age, male gender, and mean aortic pressure gradient were significantly related to aortic dilatation, predominantly at the aortic root. Coarctation, systemic hypertension, and GCS at annulus were not predictive. Importantly, 25 patients with moderate AR have a significantly higher sinus of Valsalva diameter (34.5 $\pm$ 5.5 vs. 31.6 $\pm$ 5.7 mm, $P = 0.0195$).

Dilatation of the ascending aorta (AAo) is also an important concomitant in Tetralogy of Fallot (ToF). Pontnau *et al.*[29] assessed aortic root dilatation and stiffness by CMR imaging in adults with repaired ToF. In a study of 50 ToF patients and 50 controls, standard CMR sequences obtained aortic root dimensions; aortic distensibility and PWV and examined elasticity. Compared with controls, patients with ToF had significantly decreased distensibility, increased PWV, impaired LV and RV ejection fraction, and AR was seen more often. Furthermore, no significant relationship was seen between age and distensibility, age and PWV, age at repair and stiffness or indeed age at surgical repair and aortic dilatation.

Cruz *et al.*[30] used a multimodality approach to assess the prevalence and implications of this aortic dilatation, utilizing CMR imaging to measure aortic dimensions, LV mass, systolic function, and 2D STE to derive the peak circumferential AAo Strain (CAAS) and thus calculate the aortic stiffness index. The global peak CAAS was calculated as the average peak systolic circumferential strain of the six segments representing the whole circumference of the AAo in short-axis view. Although systolic, diastolic, and pulse pressures were within normal range, a larger AAo diameter correlated with higher LV end-diastolic and end-systolic volumes, LV mass, and lower arterial stiffness (Ea) ($r = -0.34$, $P = 0.03$). There was a positive correlation between the AAo diameter measured by CMR imaging and 2D STE-derived aortic stiffness index ($r = 0.315$, $P = 0.045$). Furthermore, by multivariate analysis, age ($\beta = 0.297$, $P = 0.038$) and 2D STE aortic stiffness index ($\beta = 0.289$, $P = 0.044$) were independent predictors of the AAo diameter. The authors conclude that a multimodality approach to imaging of the AAo may unmask an intrinsic aortopathy after ToF repair.

CMR is the established gold standard when assessing RV volume, RV ejection fraction, and regurgitant fraction (RF). However, CMR is less available, more resource intensive, and costly compared with echocardiography. Silva *et al.*[31] used a standardized systematic approach of 2D transthoracic echocardiography (TTE) and 2D STE to compare echocardiographic- and CMR-derived indices in the same patients. RV mid-cavity diameter could be used to accurately predict RV end-diastolic volume, and the RV GLS showed good linear correlation with TTE and CMRI parameters of RV function.

Moving on from ToF, several authors addressed the difficult issue of imaging the single ventricle. Bellsham-Revell *et al.*[32] used TTE before and after the Hybrid Procedure first-stage surgical palliation where an unrestrictive interatrial communication is critical. The most striking echocardiographic feature of atrial restriction was the change in spectral Doppler waveform from more normal sawtooth pattern to a notched pulsatile pattern. In the adult with a palliated Fontan circulation, Castaldi *et al.*[33] used integrated multimodality investigations to assess cardiac performance. They found that standard 2D echocardiography has limited value for functional evaluation of single ventricles, but that 3D ejection fraction and speckle tracking have shown better correlation with VO_2max values. NT-pro-BNP levels showed a strong correlation with longitudinal strain and 3D ejection fraction. Cordina *et al.*[34] looked at echocardiographic predictors of mortality in this complex group of adults with CHD and a Fontan circulation. After examining many standard echocardiographic indices of ventricular performance, they reported that an increased ratio of the systolic-to-diastolic duration (>1.1) measured using inflow Doppler across the dominant atrioventricular valve was the most important echocardiographic marker and should be incorporated into routine clinical assessment.

Finally in the Young Investigator Award—Basic Science oral presentation, Valverde *et al.*[35] presented results from a European multicentre assessment of the feasibility and accuracy of 3D printed models in complex CHD in newborns and children (*Figure 4*). After

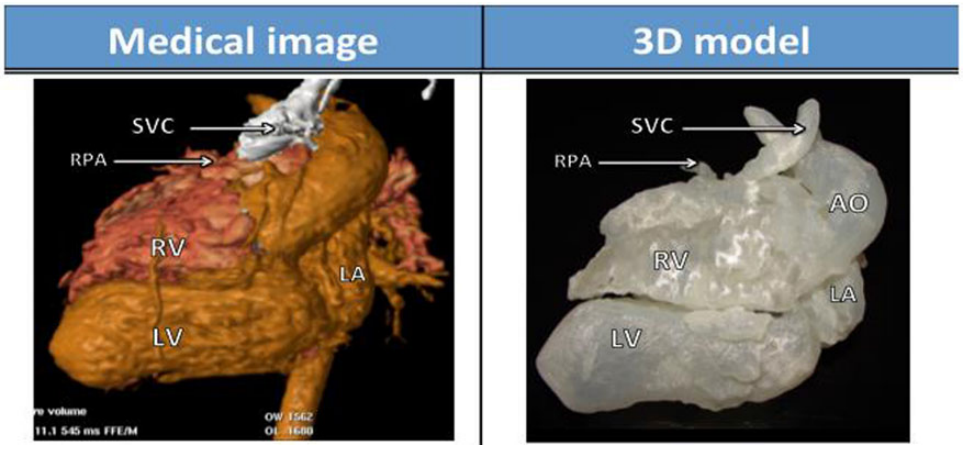

Figure 4 Example of 7.5-year-old boy with dextrocardia double outlet right ventricle, sub aortic ventricular septal defect, and severe pulmonary stenosis with previous bi-directional cavopulmonary connection. The patient was considered for Fontan completion, but the bi-ventricular repair was also considered. 3D model helped to exclude the option of biventricular repair due to the small RV size.

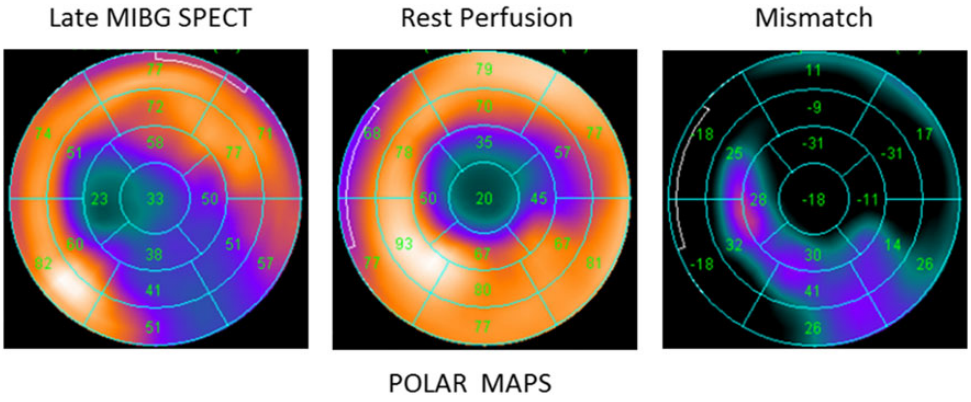

Figure 5 Polar maps representing regional left ventricular myocardial innervation (late MIBG uptake, left panel) and perfusion (middle panel). Mismatch is defined as a myocardial region with reduced late MIBG uptake despite preserved perfusion (right panel).

reporting anatomic and morphologic accuracy compared with CMR/computed tomography and actual surgical exploration, they then reported the effect of having 3D printed heart models on surgical decision-making. There was wide acceptance by the involved cardiologists and cardiac surgeons and suggest that such modelling may become the elective tool for surgical planning of complex CHD and may help reducing surgical time and surgical complications.

Nuclear cardiology and cardiac computed tomography

Single photon emission computed tomography (SPECT) is an established approach to detect myocardial ischaemia in patients with known or suspected coronary artery disease (CAD). There is increasing attention to improve the cost-effectiveness of this approach. SPECT perfusion studies are commonly based on a stress-rest protocol. In case of normal stress imaging results, a rest acquisition could be safely avoided as demonstrated in a large population of patients with a wide range of pre-test likelihood of disease by Kitsiou *et al.*,[36] thus lowering radiation exposure, costs, and exam time. On the other hand, it is known that attenuation artifacts may induce false-positive stress SPECT results. Lagan *et al.*[37] demonstrated that new SPECT scanners, with ECG gating and in-built CT to correct for diaphragm/breast attenuation, allow to detect less reversible perfusion defects resulting in lower referral to invasive coronary angiography, significant cost savings without compromising patients' safety.

Nuclear imaging of cardiac innervation by (123)I-metaiodobenzylguanidine (^{123}I-MIBG) is able to assess abnormal cardiac sympathetic activity in patients with HF and has established prognostic implications. Rio *et al.*[38] studied 102 patients with HF prior to cardiac

resynchronization therapy (CRT). Increased cardiac sympathetic activity at baseline, as shown by low late heart-to-mediastinum ratio of ^{123}I-MIBG uptake (<1.5), was associated with larger left ventricular volumes and worse global longitudinal strain with less improvement of functional parameters at 6 months after CRT. However, abnormal cardiac sympathetic activity after CRT can be favourably modulated by high intensity exercise training as Abreu *et al.*[39] demonstrated using the same imaging approach. ^{123}I-MIBG and myocardial perfusion SPECT imaging, when combined in patients with HF, provide additional prognostic information. In patients with LV ejection fraction <35%, Limeres *et al.*[40] demonstrated that both inducible ischaemia and a 'mismatch' pattern, i.e. lower ^{123}I-MIBG uptake in the presence of preserved perfusion (*Figure 5*), were powerful predictors of major adverse cardiovascular events at 35 months.

Detection of inflammation is a recent specific application of nuclear imaging. Becoulet *et al.*[41] studied a small series of 17 consecutive patients with suspected inflammatory cardiomyopathies by ^{18}F-FDG positron emission tomography. Six patients had the final diagnosis of cardiac sarcoidosis (CS), and all had positive PET scans with distinctive features compared with the seven non-CS patients with mildly positive PET scans. All patients with positive PET scans had evidence of late gadolinium enhancement by magnetic resonance in FDG uptake areas, suggesting a true positivity of PET for the presence of myocardial inflammation.

The clinical use of coronary CT angiography (CCTA) has been expanded from diagnosis of CAD to prognostic stratification, and thanks to recent technological advancements, the radiation exposure to the patient has been substantially reduced. Clerc *et al.*[42] followed for a median period of 6.1 years, 434 patients studied by low-dose 64-slice CCTA (mean effective dose 1.7 $\pm$ 0.6 mSv). No major adverse cardiovascular event (MACE) occurred in the 153 patients with normal coronary arteries at CTA while MACE were registered in a progressively greater proportion of patients with non-obstructive, obstructive, or already revascularized coronary lesions. Thus, CCTA suggested a warranty period of >6 years for patients with normal coronaries. Non-obstructive CAD deserves specific attention since it may be at risk of atherothrombotic events. In a large population of 761 patients with angina symptoms who underwent 128-row multislice CCTA, Jug *et al.*[43] demonstrated that, after adjustment for age, gender, and risk factors, non-obstructive CAD was associated with a significant increase in the risk of adverse events, compared with no CAD, with an annual event rate of 2.8%.

Relevant applications of CT include characterization of cardiac anatomy before interventional procedures or in structural cardiac diseases. Pontone *et al.*[44] showed that CT imaging of the left atrium may improve outcome of radiofrequency catheter ablation of atrial fibrillation and can now be obtained with an effective dose of <1 mSv, close to chest X-ray exposure. Celeng *et al.*[45] showed a better reproducibility of CT angiography to measure aortic root dimensions in 101 twin pairs compared with transthoracic echocardiography and found that the heritability of the aortic root geometry is stronger than it was reported previously. Finally, Van Den Hoven *et al.*[46] used CT to evaluate the prevalence of partial abnormal pulmonary venous return (PAPVR) in 90 patients with Turner syndrome. A quarter of all Turner patients turned out to have PAPVR, which was missed before in nearly half of the patients suggesting that pulmonary venous return should be implemented in the standard imaging protocol of Turner patients.

Conflict of interest: None declared.

References

1. Gargani L, Pang PS, Miglioranza M, Landi P, Dini FL, Picano E. The prognostic value of lung ultrasound at discharge in heart failure. *Eur Heart J Cardiovasc Imaging* 2015;**16**(Suppl. 2):S1–3.
2. Garcia Martin A, Moya-Mur JL, Carbonell-San Roman SA, Rodriguez-Munoz D, Garcia-Lledo A, Casas-Rojo E *et al.* Right ventricular global longitudinal strain provides higher prognostic value than right free wall longitudinal strain in patients with left heart disease. *Eur Heart J Cardiovasc Imaging* 2015;**16**(Suppl. 2):S15–42.
3. Duchenne J, Turco A, Claus P, Vunckx K, Pagourelias E, Rega F *et al.* Relationship of FDG-PET and pressure-strain loops as novel measures of regional myocardial workload in LBBB-like dyssynchrony. *Eur Heart J Cardiovasc Imaging* 2015;**16**(Suppl. 2):S1–3.
4. Galli E, Fournet M, Samset E, Leclercq C, Donal E. Left ventricular mechanics: novel tools to evaluate function and dyssynchrony in controls and cardiac resynchronization therapy candidates. *Eur Heart J Cardiovasc Imaging* 2015;**16**(Suppl. 2):S130–2.
5. Muraru D, Siciliano M, Migliore F, Cavedon S, Folino F, Pedrizzetti G *et al.* Cardiac resynchronization therapy by multipoint pacing improves the acute response of left ventricular mechanics and fluid dynamics: a three-dimensional and particle image velocimetry echocardiographic study. *Eur Heart J Cardiovasc Imaging* 2015;**16**(Suppl. 2):S102–29.
6. Sade LE, Bal U, Eroğlu S, Pirat B, Müderrisoğlu H. Speckle tracking strain correlates better with functional capacity and hemodynamic burden than ejection fraction in patients with severe heart failure. *Eur Heart J Cardiovasc Imaging* 2015;**16**(Suppl. 2):S15–42.
7. Kosmala W, Rojek A, Przewlocka-Kosmala M, Karolko B, Mysiak A, Marwick TH. Blunted increase in LV longitudinal deformation during exercise contributes to the transition from an asymptomatic stage to clinically overt HFpEF. *Eur Heart J Cardiovasc Imaging* 2015;**16**(Suppl. 2):S15–42.
8. Sanchez-Martinez S, Duchateau N, Erdei T, Fraser A, Bijnens BH, Piella G. Can machine learning help to identify heart failure with preserved ejection fraction? *Eur Heart J Cardiovasc Imaging* 2015;**16**(Suppl. 2):S15–42.
9. Schwartz SL, Rozenbaum RZ, Topilsky Y. Impact of tricuspid regurgitation and right ventricular dysfunction on outcome of patients undergoing trans-catheter aortic valve replacement. *Eur Heart J Cardiovasc Imaging* 2015;**16**(Suppl. 2):ii43.
10. Del Val Martin D, Fraile Sanz C, Salido Tahoces L, Hernandez-Antolin R, Fernandez-Golfin C, Mestre Barcelo JL *et al.* Significant mitral regurgitation evolution in patients with severe aortic stenosis after transcatheter aortic valve implantation (TAVI): results and prognostic implications. *Eur Heart J Cardiovasc Imaging* 2015;**16**(Suppl. 2):ii44.
11. Szymanski P, Hryniewiecki T, Jastrzebski J, Dabrowski M, Sorysz D, Kochman J *et al.* An impact of pre- and postprocedural mitral regurgitation on mortality following TAVI. *Eur Heart J Cardiovasc Imaging* 2015;**16**(Suppl. 2):ii44.
12. Casalta AC, Galli E, Szymanski C, Salaun E, Lavoute C, Haentjens J *et al.* Prognostic value of LV global longitudinal strain in aortic stenosis with preserved LV ejection fraction. *Eur Heart J Cardiovasc Imaging* 2015;**16**(Suppl. 2):ii109.
13. Tang Z, Jin CN, Tang H, Fan K, Kam K, Yan BP *et al.* Impaired presystolic contraction and saddle-shape deepening of mitral annulus contributes to atrial functional regurgitation: a three-dimensional echocardiographic study. *Eur Heart J Cardiovasc Imaging* 2015;**16**(Suppl. 2):ii84.
14. Villemain O, Kwiecinski W, Bel A, Robin J, Bruneval P, Arnal B *et al.* Non-invasive ultrasonic chordal cutting. *Eur Heart J Cardiovasc Imaging* 2015;**16**(Suppl. 2):ii47.
15. Bertrand PB, Dezutter T, Debusschere N, Vrolix M, Claus P, Verdonck P *et al.* Virtual 3D modeling of the mitral valve. *Eur Heart J Cardiovasc Imaging* 2015;**16**(Suppl. 2):ii211.
16. Gurzun MM, Rosca M, Calin A, Beladan C, Serban M, Ginghina C *et al.* Dynamic changes of mitral annulus shape in different types of mitral valve prolapse. A three-dimensional transoesophageal study. *Eur Heart J Cardiovasc Imaging* 2015;**16**(Suppl. 2):ii37.
17. Aquila I, Fernandez-Golfin C, Gonzalez A, Rincon LM, Hinojar R, Garcia A *et al.* Fully-automated software for mitral valve assessment in chronic mitral regurgitation by three-dimensional transesophageal echocardiography. *Eur Heart J Cardiovasc Imaging* 2015;**16**(Suppl. 2):ii95.
18. Ladeiras-Lopes R, Sampaio F, Fonseca P, Fontes-Carvalho R, Pinho M, Campos AS *et al.* Proximal flow convergence by 3D echocardiography in the evaluation of mitral valve area in rheumatic mitral stenosis. *Eur Heart J Cardiovasc Imaging* 2015;**16**(Suppl. 2):ii203.

19. Di Salvo G, Issa Z, Moiduddin N, Siblini G, Bulbul Z. Normal range of left ventricular strain, dimensions and ejection fraction using three-dimensional speckle-tracking echocardiography in neonates. *Eur Heart J Cardiovasc Imaging* 2015;**16**(Suppl. 2):ii98.
20. Vieira MS, Kowallick J, Rafiq I, Chabiniok R, Figueroa A, Carr R *et al.* Occult anthracycline cardiac injury in adolescents and young adults cancer survivors with normal left ventricular ejection fraction. *Eur Heart J Cardiovasc Imaging* 2015;**16**(Suppl. 2): ii150.
21. Nastase OA, Amzulescu M, Boileau L, Page M, de Meester C, Boulif J *et al.* Diffuse myocardial fibrosis quantification by magnetic resonance imaging in patients with aortic valve diseases. *Eur Heart J Cardiovasc Imaging* 2015;**16**(Suppl. 2):ii150.
22. von Knobelsdorff F, Hennig P, Menza M, Dieringer MA, Foell D, Jung B *et al.* Abnormal regional myocardial motion in patients with left ventricular pressure overload detected by MR tissue phase mapping at rest and during stress. *Eur Heart J Cardiovasc Imaging* 2015;**16**(Suppl. 2):ii152.
23. Castillo E, Maceira A, Llopis A, Velez O, Tebar L. Potential utility of splenic switch-off to improve the diagnostic performance of vasodilator stress cardiac magnetic resonance. *Eur Heart J Cardiovasc Imaging* 2015;**16**(Suppl. 2):ii152.
24. Kim KJ, Park JB, Kim HK, Yoon YE, Lee SP, Kim YJ *et al.* Prognostic value of cardiac magnetic resonance for preoperative assessment of patients with severe functional tricuspid regurgitation. *Eur Heart J Cardiovasc Imaging* 2015;**16**(Suppl. 2):ii134.
25. Ramos V, Silva J, Ferreira ND, Bettencourt B, Gama V. Can blunted heart rate response to adenosine vasodilator stress have prognostic implications on myocardial perfusion imaging by cardiovascular magnetic resonance? *Eur Heart J Cardiovasc Imaging* 2015;**16**(Suppl. 2):ii151.
26. Aguiar Rosa S, Galinho A, Moura Branco L, Timóteo AT, Agapito A, Sousa L *et al.* Predictors of aortic dilation in patients with bicuspid aortic valve. *Eur Heart J Cardiovasc Imaging* 2015;**16**(Suppl. 2):ii149.
27. Necas J, Kovalova S. Mechanisms of regurgitation in bicuspid aortic valve. *Eur Heart J Cardiovasc Imaging* 2015;**16**(Suppl. 2):ii233.
28. Miśkowiec D, Kasprzak JD, Lipiec P. Does the morphology of bicuspid aortic valve influence aortic diameter? A meta-analysis. *Eur Heart J Cardiovasc Imaging* 2015; **16**(Suppl. 2):ii148.
29. Pontnau F. Aortic root dilatation and stiffness assessed by magnetic resonance imaging in adults with repaired tetralogy of Fallot. *Eur Heart J Cardiovasc Imaging* 2015; **16**(Suppl. 2):ii71.
30. Cruz C, Pinho T, Madureira AJ, Lebreiro A, Dias CC, Ramos I *et al.* Multimodality assessment of the ascending aorta after tetralogy of Fallot repair. *Eur Heart J Cardiovasc Imaging* 2015;**16**(Suppl. 2):ii57.
31. Silva T, Agapito A, de Sousa L, Oliveira JA, Branco LM, Timóteo AT *et al.* Accurate echocardiographic parameters for the evaluation of adult patients with repaired tetralogy of Fallot: validation with cardiac magnetic resonance imaging. *Eur Heart J Cardiovasc Imaging* 2015;**16**(Suppl. 2):ii147.
32. Bellsham-Revell H, Peacock K, Pushparajah K, Miller OI, Simpson JM. The left pulmonary artery Doppler in the assessment of atrial restriction after the hybrid procedure for hypoplastic left heart syndrome. *Eur Heart J Cardiovasc Imaging* 2015; **16**(Suppl. 2):ii58.
33. Castaldi B, Romanato S, Callegari A, Bernardinello V, Reffo E, Milanesi O. Integrated imaging to evaluate cardiac performance in Fontan patients. *Eur Heart J Cardiovasc Imaging* 2015;**16**(Suppl. 2):ii147.
34. Cordina R, von Klemperer K, Kempny A, Senior R, Celermajer D, Babu-Narayan S *et al.* Echocardiographic predictors of mortality in adults with a Fontan circulation. *Eur Heart J Cardiovasc Imaging* 2015;**16**(Suppl. 2):ii56.
35. Valverde I, Gomez G, Suarez-Mejias C, Hosseinpour AR, Hazekamp M, Gonzalez-Calle A *et al.* 3D printed models for surgical planning in complex Congenital Heart Disease. *Eur Heart J Cardiovasc Imaging* 2015;**16**(Suppl. 2):ii46.
36. Kitsiou A, Papanikolaou S, Grironiou K, Antonopoulos M, Mpouki M, Moustakas G *et al.* Stress-only normal SPECT myocardial perfusion imaging: is it enough? *Eur Heart J Cardiovasc Imaging* 2015;**16**(Suppl. 2):ii13.
37. Lagan J, Meah M, Hasleton J, Mcshane J, Trent R. Improving the cost-effectiveness of chest pain investigations using single photon emission computed tomography. *Eur Heart J Cardiovasc Imaging* 2015;**16**(Suppl. 2):ii48.
38. Rio P, Abreu A, Santos V, Santa-Clara H, Oliveira L, Martins Oliveira M *et al.* Is autonomic nervous dysfunction severity associated to less benefit from cardiac resynchronization therapy? *Eur Heart J Cardiovasc Imaging* 2015;**16**(Suppl. 2):ii48.
39. Abreu A, Santa Clara H, Santos V, Oliveira L, Oliveira M, Rio P *et al.* Autonomic nervous system modulation in patients with heart failure and resynchronization after high intensity interval training. *Eur Heart J Cardiovasc Imaging* 2015;**16**(Suppl. 2):ii49.
40. Limeres Freire J, Rodriguez J, Oristrell G, Quiroga X, Pizzi N, Perez-Rodon J *et al.* Nuclear imaging to predict adverse events in heart failure patients. *Eur Heart J Cardiovasc Imaging* 2015;**16**(Suppl. 2):ii49.
41. Becoulet L, Guijarro D, Pallardy A, Mathieu C, Valette F, Gueffet JP *et al.* FDG-PET imaging in suspected inflammatory cardiomyopathies: comparison with the classical pattern of cardiac sarcoidosis and impact on diagnosis. *Eur Heart J Cardiovasc Imaging* 2015;**16**(Suppl. 2):ii13.
42. Clerc OF, Kaufmann BP, Possner M, Liga R, Vontobel J, Mikulicic F *et al.* Long-term prediction of cardiac events using low-dose coronary ct angiography with prospective triggering. *Eur Heart J Cardiovasc Imaging* 2015;**16**(Suppl. 2):ii49.
43. Jug B, Kosuta D, Fras Z. Prognostic impact of non-obstructive coronary artery disease on coronary computed tomographic angiography: a single-center study. *Eur Heart J Cardiovasc Imaging* 2015;**16**(Suppl. 2):ii209.
44. Pontone G, Andreini D, Annoni A, Petulla M, Russo E, Innocenti E *et al.* Submillisievert computed tomography with model-based iterative reconstruction before pulmonary veins radiofrequency catheter ablation of atrial fibrillation: impact on radiation exposure and outcome. *Eur Heart J Cardiovasc Imaging* 2015;**16**(Suppl. 2):ii12.
45. Celeng C, Kolossvary M, Kovacs A, Szilveszter B, Molnar A, Horvath T *et al.* Impact of imaging modality on the heritability estimates of aortic root geometry: a classical twin study. *Eur Heart J Cardiovasc Imaging* 2015;**16**(Suppl. 2):ii12.
46. Van Den Hoven AT, Saru-Chelu RG, Duijnhouwer AL, Van Hagen IM, Roos-Hesselink JW. Evaluation of PAPVR using cardiac CTor MR imaging in patients with Turner syndrome. *Eur Heart J Cardiovasc Imaging* 2015;**16**(Suppl. 2):ii50.